THE JOURNAL OF PHYSICAL CHEMISTRY A
A JOURNAL OF THE AMERICAN CHEMICAL SOCIETY

pubs.acs.org/JPCA Article

Comparison of RNC Coupling and CO Coupling Mediated by Cr−Cr Quintuple Bond and B−B Multiple Bonds: Main Group Metallomimetics

Published as part of The Journal of Physical Chemistry virtual special issue "Alexander Boldyrev Festschrift".

Sagar Ghorai, Raghavendra Meena, Anju P. Joseph, and Eluvathingal D. Jemmis*

Cite This: *J. Phys. Chem. A* 2021, 125, 7207−7216 Read Online

ACCESS | Metrics & More | Article Recommendations | Supporting Information

ABSTRACT: A theoretical analysis of reductive coupling of isocyanide and CO mediated by a Cr−Cr quintuple bonded complex and B−B multiple bonded complexes shows how the difference in donor−acceptor capability of isocyanide and CO ligands controls the product distributions. In the case of CO, the Cr−Cr quintuple bonded complex is unable to show C−C coupling due to the high π- back bonding possibility of CO and the reaction follows the singlet potential energy surface throughout, whereas, in the case of isocyanide, less π- back bonding possibility allows the reactions to undergo a spin transition and gives a series of products with different spin multiplicities. Similarly, reactions of B−B multiple bonded complexes with CO and isocyanides are also controlled by donor−acceptor capabilities of ligands, and the C−C coupling takes place by changing the oxidation state of the boron centers from +I to +II, in contrast to the classical main group mediated reactions where stable oxidation states are always preserved. This part of the main group chemistry which is dominated by donor−acceptor bonding interaction is more likely to follow transition metal behavior.

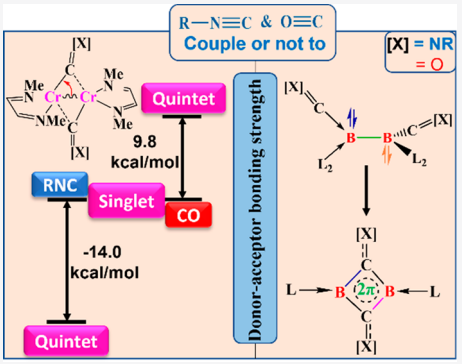

INTRODUCTION

Combining small molecules to yield complex chemical architectures has always been of immense interest in chemistry. Multiple bonded complexes which are store houses of electrons form unusually effective templates to orchestrate reductive coupling of small molecules and contribute to this endeavor.[1−4] Understanding the nature of chemical bonds and their relationship to reactivity helps in such design. Often dramatic differences in reactivity are brought in by small changes in the ligands and substituents, and here we present a computational study of one such example from the literature. In 2014, Theopold has shown that the Cr−Cr quintuply bonded complex, ^{1}**1a**, undergoes coupling reactions with isocyanide to give ^{1}**2a**, ^{7}**3a**, and ^{7}**4a**, with an excess of CyNC (Scheme 1a) and ^{5}**5a** with 4 equiv of isocyanide.[3] In contrast, a related small molecule CO leads to just one product (^{1}**6a**) with the same Cr_2 complex.[4,5] The reaction of ^{1}**1b** with isocyanide involves many intersystem crossings to give products with different spin multiplicities.[5] Complex ^{1}**2b**, the major product (40%) of excess isocyanide treatment, is a kinetically controlled product.[5] A mechanistic bifurcation from the reactant singlet surface to higher spin states is due to higher exchange stabilizations.[5] In contrast, the same quintuply bonded complex was unable to show any coupling reaction with the isoelectronic carbon monoxides.[6] We focus on the ways in which this difference in reactivity of two similar molecules relates to the structure and bonding of different intermediates involved in the reaction. Reactions of this multiple bonded transition metal complex can be compared to the reactions of B−B multiple bonded complexes with isocyanide and CO (Scheme 1a−c)[2,4] to further the discussions on metallomimetics involving low-valent main group compounds.[7−13] B−B multiple bonded complexes bring about coupling of both isocyanide and CO.[2,4] Detailed mechanistic studies of the CO coupling reaction revealed that by varying the ligands attached to boron centers with different sigma donors and pi acceptors, the coupling reaction can be controlled.[14,15] In order to understand the CO activation mechanism, Mo and co-workers analyzed the addition of the first molecule of CO to the diboryne system using a block localized wave function method.[16] It was shown that the diboryne complex mimics the transition metal behavior in the activation of CO, i.e, HOMO−LUMO swap without photoinduction. Although there have been several studies of this reaction, the variation of bonding at the rate-

Received: June 12, 2021
Revised: August 1, 2021
Published: August 17, 2021

Scheme 1. (a) Reactivity of Cr−Cr Quintuple Bonded Complex 1 with Isocyanide and CO. Table Shows the Combination of Ligands and Substituents in the Experimental Study and Model Complexes Chosen for the Present Study. (b) Reactivity of B−B Triple Bonded Complex 7 with Isocyanide and CO. (c) Reactivity of Boraallene Complex with Isocyanide

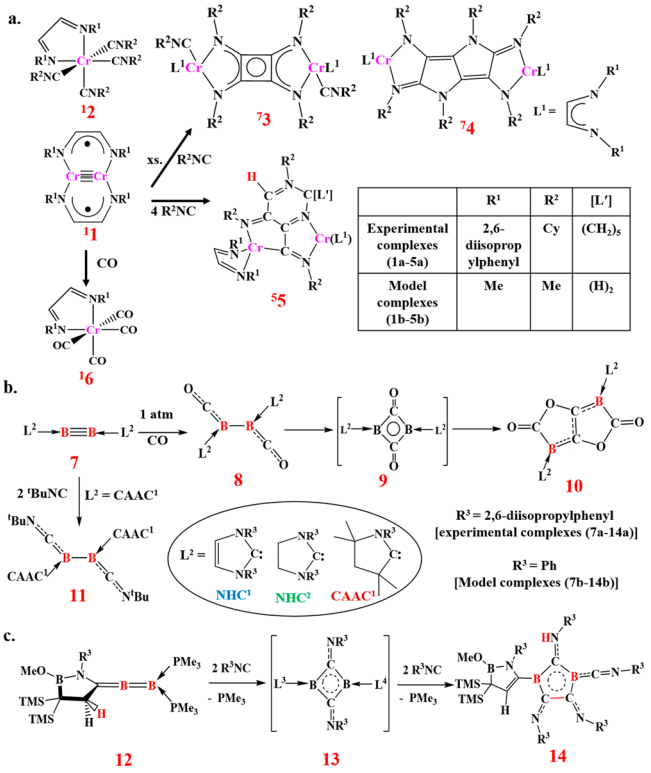

	R¹	R²	[L']
Experimental complexes (1a-5a)	2,6-diisopropylphenyl	Cy	$(CH_2)_5$
Model complexes (1b-5b)	Me	Me	$(H)_2$

determining step (**8** to **9**) and the driving force for the C−C coupling reaction have not been analyzed in greater detail. Continuing our efforts to compare chemistry across the periodic table, we investigate the differences in the mechanistic details for isocyanide reactions, **7** to **11**[17] and **12** to **14**,[4] and compare these to similar reactions of quintuply bonded Cr2 complexes. The orbital evolution along the IRC of the rate-determining step and C−C coupling step is analyzed by invoking the intrinsic bond orbital (IBO) representation of the wave function to provide further insight into the problem.[18,19] Specifically, we examine the difference between classical coupling reactions that takes place by maintaining the stable oxidation states throughout[20−22] and coupling by low valent main group compounds where the change of oxidation state and a donor−acceptor model is more appropriate akin to transition metals.[23,24] Such detailed understanding helps us to push the limits from one end to the other end of the spectrum.

COMPUTATIONAL DETAILS

All the calculations are carried out using the Gaussian 09 program package, version D.[25] Geometry optimization for the transition metal complexes is carried out using the M06L functional[26,27] with the LANL2DZ basis set for Cr and the 6-31G(d) basis set for all the other elements (C, H, N, and O). In order to decrease the computational cost, bulky groups (2,6-diisopropylphenyl and cyclohexyl) are modeled by the methyl group for Cr2-complexes (Scheme 1a) and 2,6-diisopropyl-phenyl is modeled by the phenyl group for B2-complexes (Scheme 1b and 1c). In order to make comparison between isocyanide coupling and CO coupling and due to the involvement of several high spin intermediates during the reaction for isocyanide coupling, we avoid the use of hybrid functionals which overstabilize the high spin states. The stability of the wave function for all the complexes and

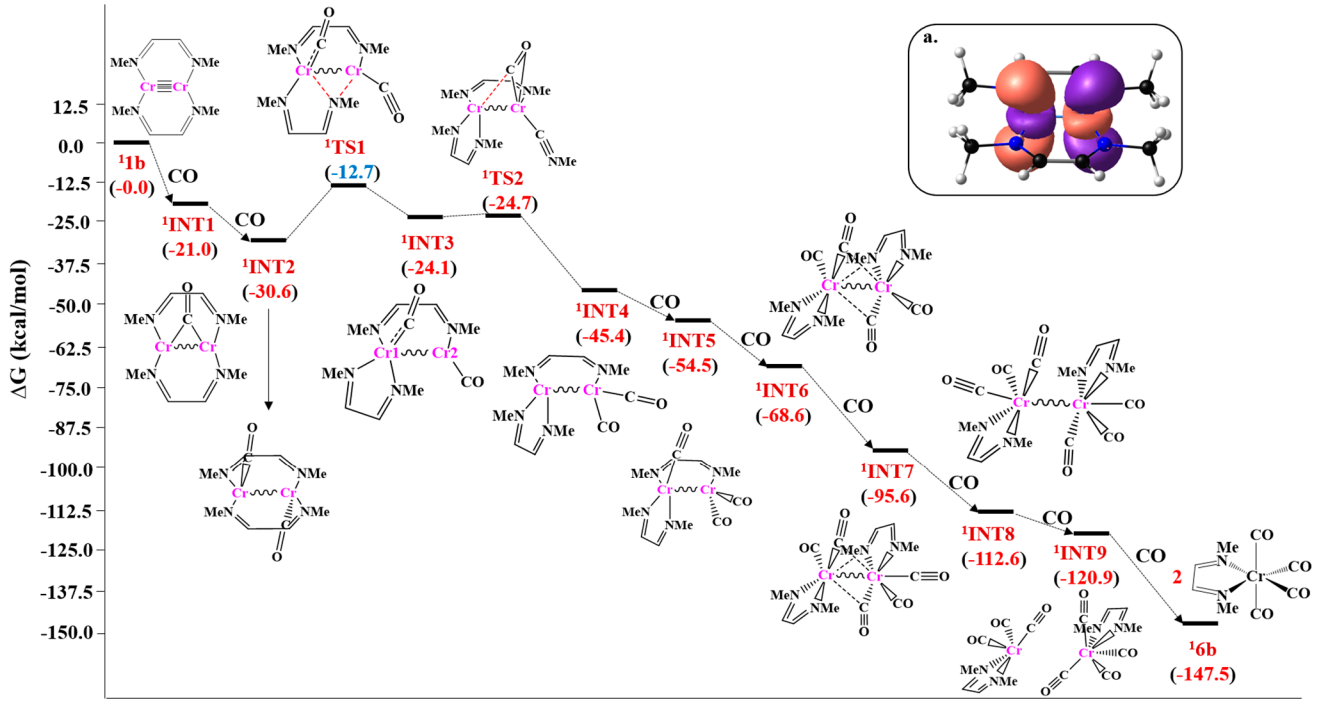

Figure 1. Free energy (kcal/mol) profile diagram for the formation of ^{1}**6b** starting from ^{1}**1b** at the M06-L level of theory with the LANL2DZ basis set for Cr and the 6-31G(d) basis set for all other atoms. The zero energy of ^{1}**1b** includes the energies of the eight CO groups: (a) HOMO of ^{1}**1b**.

https://doi.org/10.1021/acs.jpca.1c05185
J. Phys. Chem. A 2021, 125, 7207−7216

Scheme 2. Composite Diagram with Free Energy Values (kcal/mol) for the Reaction of ^{1}1b with CO ([X] = O; color code-red) and Methyl Isocyanide ([X] = NMe; color code-blue) at the M06-L Level of Theory with the LANL2DZ Basis Set for Cr and the 6-31G(d) Basis Set for All Other Atoms. ^{5}INT13 Is Not a Minimum When [X] = O

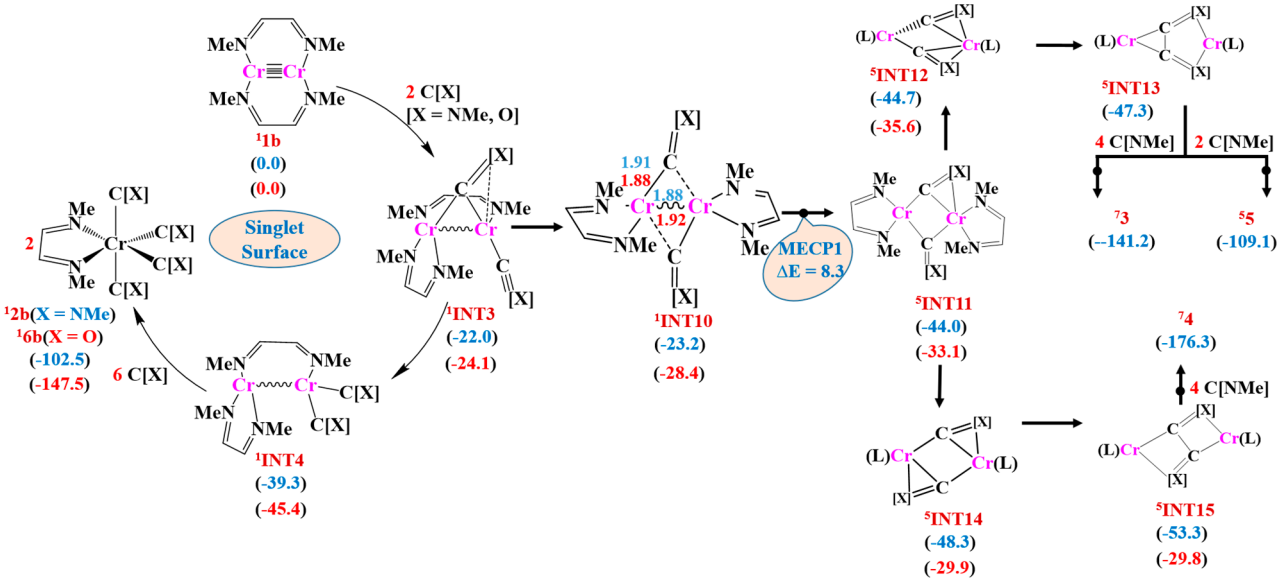

intermediates is checked using "stable = opt" and "guess = mix" keywords as implemented in Gaussian. Geometry optimization for the main group complexes is carried out using the B3LYP functional with the 6-31G(d) basis set for all the elements and the IEFPCM solvation model with toluene solvent. The nature of stationary points is examined by vibrational frequency calculations at the same level of theory.

Fragment molecular orbital (FMO) analysis and energy decomposition analysis (EDA)[28] have been carried out with the ADF program package[29] using the MO6L functional on the optimized (Gaussian 09) structures and the TZP basis set for all the atoms. Metal−ligand interactions are analyzed with the energy decomposition scheme ETS. The interaction energy is composed of three components:

$$\Delta E_{int} = \Delta E_{elstat} + \Delta E_{pauli} + \Delta E_{orb}$$

ΔE_{elstat} is the electrostatic interaction energy between the fragments calculated with a frozen electron density distribution in the given input geometry. ΔE_{pauli} is the repulsive four-electron interaction between occupied orbitals. ΔE_{orb} is an estimate of the covalent contributions to the bonding. Further, an estimate of bonding and back-bonding components to the E_{orb} was obtained by using the constrained-space orbital variation (CSOV) procedure by selectively removing fragment orbitals from the basis set of the molecule.

In order to understand the electron flow, the orbital evolution was analyzed by invoking the intrinsic bond orbital (IBO) representation of the wave function.[18,19] IBOs at each point are computed considering model complexes at the B3LYP/def2-TZVP level of theory using the Gaussian 09 program package, Version-D. Intrinsic reaction coordinate (IRC) calculations are carried out at the same level of theory. Orbital coefficients are generated at each point of the IRC using the Gaussian 09 program package. Intrinsic bond orbitals (IBOs) (*iboexp* = 2) are generated using IboView by taking the orbital information generated from the Gaussian 09 program package. Further, IBO evolution for the IRC path is used for the analysis of the electron flow.

All the experimental complexes with a particular structural type are given numbers followed with the letter **a**, such as **1a**, **2a**, and so on, and model complexes with the letter **b**. Since Cr−Cr quintuple bond mediated reactions take place on different spin states, spin multiplicity is added as a left superscript to the structural number, such as ^{1}**1b**, ^{1}**2b**, and so on. Main group mediated reactions take place only on the singlet surface. Therefore, we did not mention spin states explicitly with these structures.

RESULTS AND DISCUSSION

We begin with the mechanistic study of ^{1}**1b** with CO and compared the energetics of a few important intermediates of the reactivities of ^{1}**1b** with CO and MeNC. To understand the various controlling factors which bring differences in the RNC and CO reactions, we analyze ^{1}**INT10** from where spin state change takes place with EDA-NOCV analysis using the CSOV

Table 1. EDA-NOCV Results for the Donor−Acceptor Interaction (kcal/mol) in ^{1}INT10 (X = O and NMe) and an Estimation of Bonding and Back-Bonding Components to the E_{orb} Using the Constrained-Space Orbital Variation (CSOV) Procedure by Selectively Removing Fragment Orbitals from the Basis Set of the Molecule at the M06L/TZP Level of Theory[a]

	^{1}INT10 (X = O)			^{1}INT10 (X = NMe)		
		a	b		a	b
ΔE_{int}	−61.1			−61.8		
ΔE_{Pauli}	192.1			197.4		
ΔE_{elstat}	−128.7			−147.9		
ΔE_{orb}	−124.5	−48.9	−84.2	−111.3	−48.8	−75.3
ΔE_1	−67.9	−36.6	−44.0	−68.1	−38.5	−46.1
ΔE_2	−32.6		−25.6	−18.8		−15.1
ΔE_3	−18.2		−8.8	−19.5		−9.4

[a]Fragments are CO/MeNC and the rest of the systems. a = removing all unoccupied orbitals from CX (X = O and NMe); b = removing all unoccupied orbitals from the metal fragment.

https://doi.org/10.1021/acs.jpca.1c05185
J. Phys. Chem. A 2021, 125, 7207−7216

Scheme 3. Relative Energy ΔE (ΔG) Comparison for (a) the Rate-Determining Step of the CO Coupling Reaction, 8b → 9b, and (b) the C−C Coupling Step, INT16 → INT17, at the B3LYP/6-31G(d) Level of Theory with the IEFPCM Solvation Model and Toluene Solvent

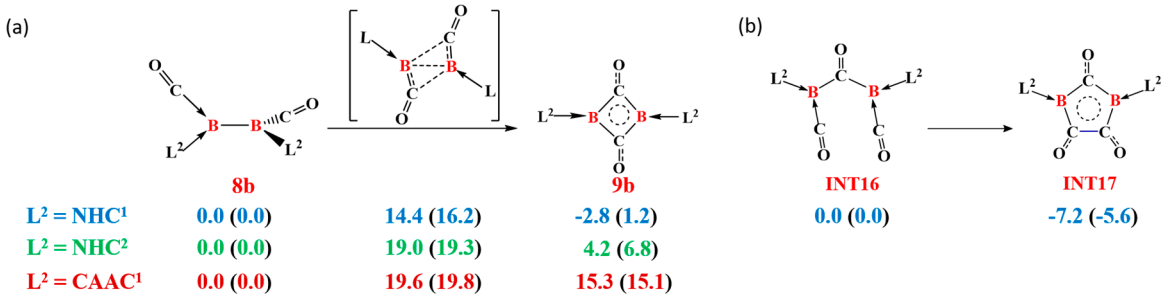

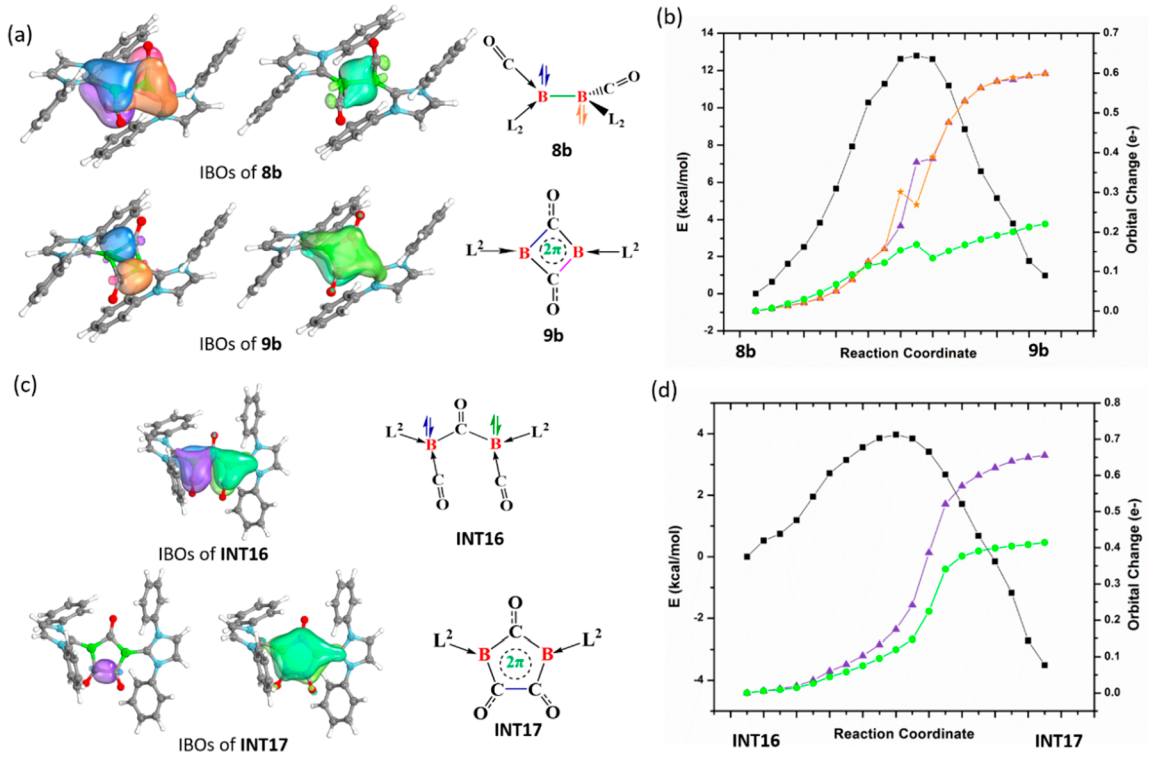

Figure 2. (a) Selected IBOs of **8b** and **9b** with their schematic description shown in the right (L^2 = NHC^1). (b) Plot of the IRC path of complexes **8b** and **9b**. Total energy changes along the path are shown using black squares at the B3LYP/def2-TZVP level of theory using the G09 software package, and IBO changes along the path are shown in green circles (the B−B σ-bond orbital in **8b** to the delocalized π-orbital in **9b**), orange asterisks (one of the boron centered lone pair orbitals stabilized by ligands in **8b** to the B−B σ-orbital in **9b**) and purple triangles (the other boron centered lone pair orbitals stabilized by ligands in **8b** to the B−B σ-orbital in **9b**) using the IboView software package. (c) IBOs of **INT16** and **INT17** (L^2 = NHC^1). (d) Plot of the IRC path of the complex for the C−C coupling reaction from **INT16** to **INT17**. Total energy changes along the path are shown using black squares at the B3LYP/def2-TZVP level of theory using the G09 software package, and IBO changes along the path are shown in green circles (one of the boron centered lone pair orbitals stabilized by ligands in **INT16** to the delocalized π-orbital in **INT17**) and purple triangles (the other boron centered lone pair orbitals stabilized by ligands in **INT16** to the B−B σ-orbital in **INT17**) using the IboView software package. [IBO changes are plotted as the root-mean-square deviation of the orbital partial charge distribution among the atoms with respect to the initial partial charge distribution.]

procedure. The reactivities of isocyanide and CO with B−B multiple complexes with the emphasis of the role of ligands to determine the reaction outcomes followed next. Finally, we compare the C−C coupling reactions mediated by classical main group complexes and borylene complexes.

Reactions of ^{1}**1b** with CO give only product ^{1}**6b** in contrast to isocyanide where singlet state to quintet and septet state crossings were possible (Scheme 1a, Figure 1).[3,6] The low energy δ*-LUMO of Cr−Cr quintuple-bonded complex ^{1}**1b** (Figure 1a) readily reacts with the high energy HOMO of CO, localized on the C end, to give ^{1}**INT1** in a highly exergonic way (−20.0 kcal/mol). The second CO addition to give ^{1}**INT2** is exergonic by 10.6 kcal/mol. Next, the diimine ligand changes its binding mode through ^{1}**TS1** to ^{1}**INT3** with a barrier height of 17.9 kcal/mol followed by shifting of CO ligand from the Cr1 center to the Cr2 center through ^{1}**TS2** to give a stable intermediate ^{1}**INT4**. Then, a series of CO additions lead to the product ^{1}**6b**. The reactivity of ^{1}**1b** toward CO (^{1}**1b** to ^{1}**6b**) and isocyanide (^{1}**1b** to ^{1}**2b**)[5] is similar on the singlet potential energy surface (Scheme 2). However, CO does not react with **1** to give equivalents of **3**−**5**. In order to understand the reluctance of intermediates involving CO in

https://doi.org/10.1021/acs.jpca.1c05185
J. Phys. Chem. A 2021, 125, 7207−7216

Scheme 4. Relative Energy ΔE (ΔG) Comparison for the Isomerization Steps of 11b (L^2 = CAAC[1]) at the B3LYP/6-31G(d) Level of Theory with the IEFPCM Solvation Model and Toluene Solvent

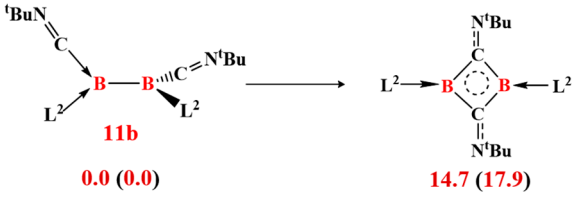

intersystem crossing which could lead to products akin to **3**−**5**, we have performed the optimization for a few selective intermediates obtained during isocyanide reactions by replacing MeNC by CO and made a comparison between them in Scheme 2. In the case of CO, the higher stability of singlet intermediate, ^{1}**INT4**, compared to quintet intermediates ^{5}**INT12** and ^{5}**INT15**, restricts the reaction to follow only the singlet pathway. For example, ^{1}**INT4** is 9.8 kcal/mol more stable than the most stable quintet intermediate, ^{5}**INT12**. This is in contrast with the MeNC coupling mechanism where higher exchange stabilization in ^{5}**INT11** allows singlet−quintet spin state crossover at **MECP1** and the most stable singlet intermediate ^{1}**INT4** lies 14.0 kcal/mol higher in energy than the most stable quintet C−C coupled intermediate ^{5}**INT15**. Though the absence of spin state crossing in the case of intermediates with CO is supported by the energetics, we analyze ^{1}**INT10** from where spin state change takes place in greater detail to understand the various controlling factors. The Cr−Cr, Cr−CO, and Cr−CNMe distances in ^{1}**INT10** give a clue to the difference in the pathways followed: the Cr−Cr distance is calculated to be longer (1.92 Å, C[X] = CO vs 1.88 Å, C[X] = CNMe) while the Cr−CO distance is shorter (1.88 Å) than the Cr−CNMe distance (1.91 Å) (Scheme 2). This change in bond length is probed by analyzing the bonding interaction between the metal fragment and one of the -C[X] (X = O, NMe) units in ^{1}**INT10** with energy decomposition analysis (EDA) and by investigation of the corresponding natural orbitals of chemical valence (NOCVs), Table 1.

The high orbital interaction (E_{orb}) for CO as ligand (−124.5 kcal/mol) compared to MeNC (−111.3 kcal/mol) suggests the ability to stabilize singlet intermediates is more when the ligand is CO. Due to the lack of symmetry in ^{1}**INT10**, the E_{orb} term cannot easily be divided into σ and π contributions separately. However, an estimate of bonding and back-bonding components to the E_{orb} was obtained by using the constrained-space orbital variation (CSOV) procedure by selectively removing fragment orbitals from the basis set of the molecule. Removal of unoccupied orbitals of CO/MeNC from the EDA calculation gives only ligand to metal bonding interactions. Similarly, removal of unoccupied orbitals of the metal fragment gives a back-bonding interaction from the metal fragment to the CO/MeNC unit, Table 1. The ligand to metal bonding interactions are almost the same for CO (48.9 kcal/mol) and MeNC (48.8 kcal/mol) ligands. The back-bonding interaction in contrast is quite high in CO (84.2 kcal/mol) compared to MeNC (75.3 kcal/mol) and constitutes a major part of the orbital interactions. Similar results are obtained by analyzing the NOCVs calculated for ^{1}**INT10** using the CSOV procedure, wherein significant changes are observed only in the ΔE_2 value having π-back-bonding character. The presence of a strong π-

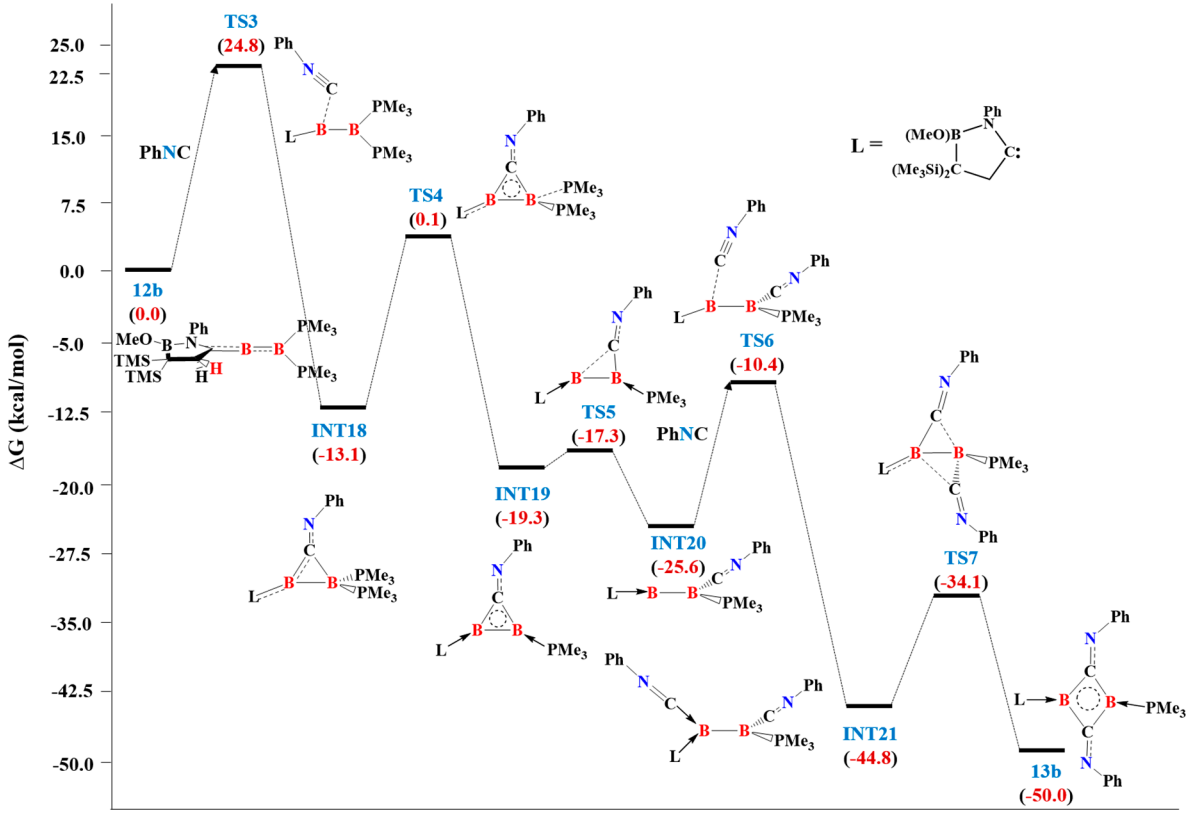

Figure 3. Free energy (kcal/mol) profile diagram for the formation of **13** starting from boraallene complex **12** at the B3LYP/6-31G(d) level of theory with the IEFPCM solvation model and toluene solvent.

https://doi.org/10.1021/acs.jpca.1c05185
J. Phys. Chem. A 2021, 125, 7207−7216

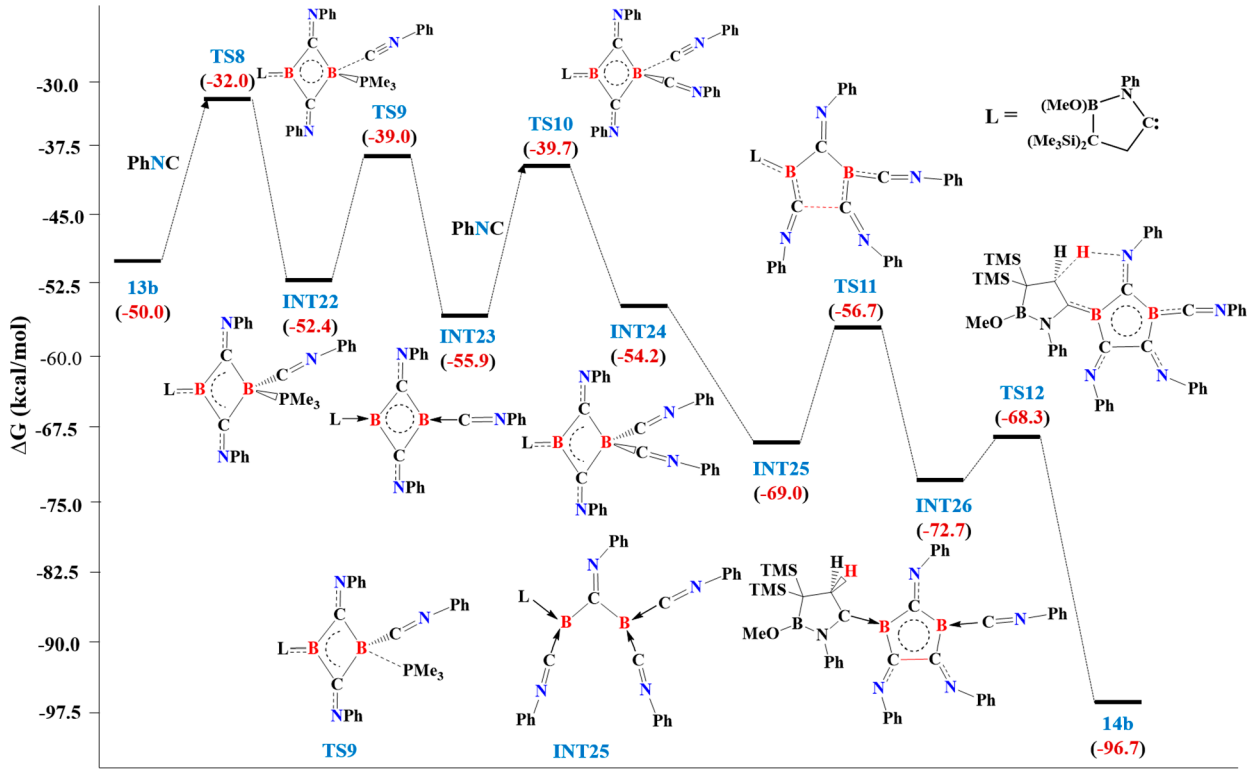

Figure 4. Free energy (kcal/mol) profile diagram for the formation of **14** starting from **13** at the B3LYP/6-31G(d) level of theory with the IEFPCM solvation model and toluene solvent.

Scheme 5. Schematic Representation of C−C Coupling Steps for Main Group Mediated CO and Isocyanide Coupling Reactions with Formal Oxidation State Assigned[a]

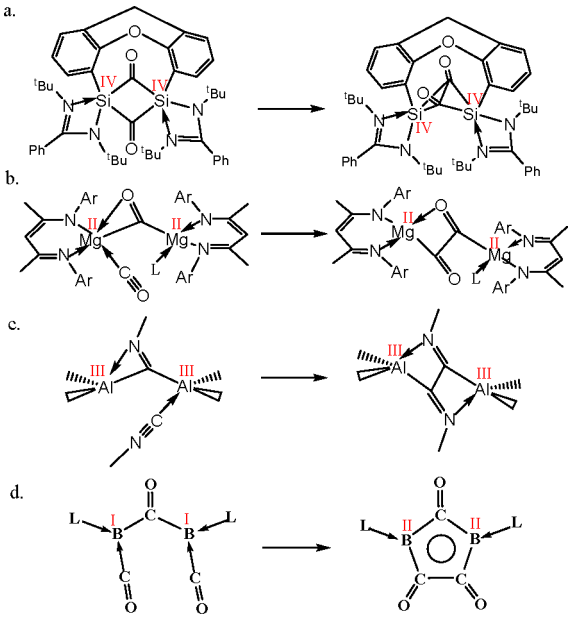

[a]For simplicity, a generic ligand scheme is used here.

back-bonding interaction in the case of CO compared to MeNC is also observed in ^{1}**INT4** (Table S1). Therefore, the strong π-back-bonding possibility in CO allows removal of the electron cloud from the Cr−Cr bonding region and provides stability toward singlet intermediates. The reduced π-back bonding in isocyanide does not provide sufficient stabilization to singlet intermediates. A spin state crossover which provides stability to the higher spin state intermediates through strong exchange interaction stabilization is a definite possibility and observed experimentally.

Previous studies highlighted a few requirements for the reductive coupling of isocyanide or CO, e.g. metal complexes with variable oxidation states, the perfect alignment of the orbitals of coupling moieties by either side-on coordination to the metal center or Lewis acid coordination or interaction of the CO unit through the O-end.[30−39] Here, we show that the fundamental difference in the donor−acceptor capabilities of isocyanide and CO distinguishes the reaction channels while reacting with ^{1}**1**.

We assessed the role of diimine ligand by calculating on a few important intermediates with bis(phenyl)-acenaphthenequinonediimine (Ph-BIAN) ligand. In both the cases, MeNC and CO, Ph-BIAN ligand stabilizes singlet intermediates more. In the case of CO, the relative energy between ^{1}**INT4** and the most stable quintet intermediate, ^{5}**INT12**, increases from 9.8 kcal/mol [L = MeN(CH)$_2$NMe] to 18.9 kcal/mol [L = Ph-BIAN] where ^{1}**INT4** is more stable. In contrast, in the case of MeNC, the relative energy between ^{1}**INT4** and the most stable quintet intermediate, ^{5}**INT15**, decreases from 14.0 kcal/mol [L = MeN(CH)$_2$NMe] to 4.7 kcal/mol [L = Ph-BIAN] where ^{5}**INT15** is more stable. Therefore, Ph-BIAN ligand may change the spin state crossing probabilities and therefore restrict the isocyanide coupling.

We also assessed the role of substituents in the isocyanide ligand by calculating on a few important intermediates with PhNC ligand. The relative energy between ^{1}**INT4** and the most stable quintet intermediate, ^{5}**INT15**, changes from 14.0 kcal/mol in the case of MeNC, to 22.0 kcal/mol in the case of PhNC, where ^{5}**INT15** is more stable. The MECP1 barriers

https://doi.org/10.1021/acs.jpca.1c05185
J. Phys. Chem. A 2021, 125, 7207−7216

between the singlet and quintet state are 8.3 and 8.7 kcal/mol for MeNC and PhNC ligands, respectively. Therefore, the substituents in the isocyanide ligand have minor effects in the spin state crossing probabilities and thus the isocyanide coupling.

The differential reactivity at the Cr−Cr quintuple bonded complex of isocyanide and CO is to be contrasted to the study of the B−B multiple bond which shows reductive coupling for both CO and isocyanide.[2,4,14] The decisive role of ligands with different σ-donating and π-accepting capabilities in stabilizing the different intermediates and thus controlling various products is described by Braunschweig et al.[14] We seek to understand this difference starting with the reported rate-determining step, conversion of **8b** (L^2 = NHC^1, N-heterocyclic Carbene) to **9b** (L^2 = NHC^1), of the CO coupling reaction (Scheme 3) and to compare it to those of the Cr2 complex.[14] For comparison, we have recalculated the energetics for all the reactions using a single level of theory (Scheme 3). It is found that a strong π-accepting ligand ($CAAC^1$)[39,40] stabilizes **8b** compared to **9b**.[40,41] Therefore, the reaction stops after the formation of **8b**. In contrast, weak π-accepting ligands (NHC^1 and NHC^2)[42−44] provide comparable stability to both bis-borylene intermediate (**8b**) and 2π-electron delocalized intermediates (**9b**). As a result, the CO coupling reaction takes place with these ligands. At first, we identify three localized orbitals: two boron centered lone pair orbitals stabilized by ligands and one B−B sigma bonding orbital (Figure 2a). IBO analysis shows that these three localized orbitals change their nature along the IRC (Figure 2b). Two boron centered lone pair orbitals become the B−C σ-bonding orbital and the B−B bonding electron pair shifted to the four membered delocalized π orbital. Therefore, **9b** is better described as a four-member ring with 2π-electron delocalization. The four-membered ring in **9b** is puckered, like other four membered 2π aromatic systems.[45−49] The aromaticity of **9b** is measured by the nuclear independent chemical shift ($NICS_{zz}$) values of −6.1 ppm at the ring center and −4.3 ppm and −16.7 ppm at 1 Å above the ring center (two values are due to the nonplanarity of the ring). This strong 2π delocalization drives the reaction in the forward direction. Similarly, IBO analysis for the C−C coupling step, **INT16** (L^2 = NHC^1) to **INT17** (L^2 = NHC^1), showed that two boron centered lone pair orbitals transform their nature during the process; one pair moved to the C−C bonding orbital, and the other pair shifted to the five-member delocalized π-orbital (Scheme 3b, Figure 2c and 2d). The π-aromaticity of **INT17** is measured by the $NICS_{zz}$ values of 4.9 ppm at the ring center and −4.3 ppm and −6.2 ppm at 1 Å above the ring center (the two values are due to the C_1 symmetry of **INT17**). Therefore, the driving force for the reductive CO coupling reaction is the stabilization of intermediates through cyclic 2π-electron delocalization. The formal oxidation state of boron changes from + I to + II on going from **8b** to **9b** and **INT16** to **INT17**.

Although isocyanide is a valence isomer of CO, homonuclear boryene complex (**7**) does not show isocyanide coupling in contrast with CO (Scheme 1b).[17] In order to understand the reluctance toward isocyanide coupling, we compared the energetics between **11b** and the cyclic intermediate obtained during CO reactions by replacing CO by ^{t}BuNC in Scheme 4. It is evident that a strong π-accepting ligand ($CAAC^1$)[39,40] stabilizes **11b** compared to the cyclic isomer. Therefore, reaction stops after the formation of **11b**. However, the Kinjo group was successful to show isocyanide coupling mediated by a bora-allene (**12**) complex (Scheme 1c).[4] Here, we study the reaction mechanism from **12b** to **14b** in detail (Figures 3 and 4). It is observed that the reaction proceeds through ligand exchange between PhNC and PMe_3 (**TS3**−**TS5**) followed by PhNC addition (**TS6**) to give the bis-borylene intermediate (**INT21**) which further isomerizes to the 2π-electron stabilized intermediate (**13b**) (Figure 3). After the formation of **13b**, the reaction proceeds through further ligand exchange between PhNC and PMe_3 (**TS8**−**TS9**) followed by PhNC addition (**TS10**) to give the bis-borylene intermediate (**INT25**) which upon C−C coupling (**TS11**) leads to the 2π-electron stabilized intermediate (**INT26**). Finally, C−H activation from **INT26** through **TS12** gives product **14b** (Figure 4). **INT21** → **13b** and **INT21** → **INT26** are similar to **8b** → **9b** and **INT16** → **INT17** of the CO coupling reaction respectively (Scheme 3a).

Changing the ligand environment from a homonuclear bis-borylene intermediate (**11b**) to a heteronuclear one (**INT21**) stabilizes the cyclic 2π intermediate (**13b**) by 5.2 kcal/mol due to the fine-tuning of the donor−acceptor interactions and drives the reaction. In particular, a strong σ-donating and very weak π-accepting ligand, PMe_3,[50] plays a decisive role for shifting the energetics. Therefore, the stabilization of cyclic intermediates with proper ligand environments is essential for the reductive coupling of CO and isocyanides. Earlier reports also show how donor−acceptor interaction plays an important role in the reactivities of low-valent group IV complexes with isocyanide and CO as ligands.[51−54] Our analysis further proves that donor−acceptor bonding is a better model for the description of low-valent (modern) main group chemistry.

In addition to boron complexes, there are Mg, Al, and Si complexes which are also capable of showing reductive CO and isocyanide couplings.[20−22] Here, we have extracted out the C−C coupling steps of all the main group mediated reactions. From an oxidation state formalism, it is found that C−C coupling reactions for Si, Mg, and Al take place by maintaining their stable oxidations states +IV, +II, and +III, respectively, as generally observed in the main group mediated reactions (Scheme 5a−5c).[20−22,55] In contrast, in the case of B, C−C coupling takes place with the change of oxidation state of B from +I to +II, a typical phenomenon observed in transition metal chemistry (Scheme 5d).

Therefore, we conclude that the recently developed modern low valent main group chemistry dominated by donor−acceptor type bonding is more likely to mimic transition metal chemistry.

CONCLUSION

We have studied the difference in reactivity of the Cr−Cr quintuple bonded complex with CO and isocyanide. A detailed mechanistic study shows that the reaction of CO follows the singlet potential energy surface throughout the reaction due to the strong π-back bonding possibility providing stability to singlet intermediate ^{1}**INT4** over the high spin state intermediates, whereas, in the case of isocyanide, less π-back bonding possibility is not sufficient to give stability to singlet intermediates and allows the reactions to undergo a spin transition at **MECP1**. The high exchange stabilization in ^{5}**INT11** allows spin state crossing at **MECP1**. Therefore, the difference in the donor−acceptor ability of CO and isocyanide decides the product distributions. Similarly, isolation of different intermediates in the reactions of B−B multiple

https://doi.org/10.1021/acs.jpca.1c05185
J. Phys. Chem. A 2021, 125, 7207−7216

bonded complexes with CO and isocyanides is also controlled by donor−acceptor capabilities of ligands. The rate-determining step and C−C coupling steps of all the reactions involve change in the electronic configuration from the boron center lone pair to the cyclic intermediates with 2π delocalization. Boron centers change their oxidation state from +I to +II in contrast to the classical main group mediated reactions where stable oxidation states are always preserved. Therefore, this part of the main group chemistry which is dominated by donor−acceptor bonding interaction is more likely to follow transition metal behavior.

However, Braunschweig et al. recently highlighted that although borylenes show similarities to transition metals, they retain main group character for the reductive coupling of N_2, the valence isomer of isocyanide and CO.[56,57] A comparison of reductive coupling of isocyanide and CO with N_2 mediated by transition metals and main group compounds is under investigation in our group.

■ ASSOCIATED CONTENT

Supporting Information

The Supporting Information is available free of charge at https://pubs.acs.org/doi/10.1021/acs.jpca.1c05185.

EDA-NOCV analysis of ^{1}**INT4** and Cartesian coordinate of the studied complexes (PDF)

■ AUTHOR INFORMATION

Corresponding Author

Eluvathingal D. Jemmis − *Inorganic and Physical Chemistry Department, Indian Institute of Science, Bangalore 560012, India*; orcid.org/0000-0001-8235-3413; Email: jemmis@iisc.ac.in

Authors

Sagar Ghorai − *Inorganic and Physical Chemistry Department, Indian Institute of Science, Bangalore 560012, India*

Raghavendra Meena − *Inorganic and Physical Chemistry Department, Indian Institute of Science, Bangalore 560012, India*

Anju P. Joseph − *Inorganic and Physical Chemistry Department, Indian Institute of Science, Bangalore 560012, India*

Complete contact information is available at: https://pubs.acs.org/10.1021/acs.jpca.1c05185

Notes

The authors declare no competing financial interest.

■ ACKNOWLEDGMENTS

We thank Supercomputer Education and Research Centre, IISc and CMSD, University of Hyderabad for computational facilities. S.G. thanks IISc for a research fellowship. E.D.J. thanks SERB-DST for funding through the Year of Science Chair Professorship.

■ REFERENCES

(1) Liddle, S. T. *Molecular Metal-Metal Bonds: Compounds, Synthesis, Properties.*; Wiley, 2015.

(2) Braunschweig, H.; Dellermann, T.; Dewhurst, R. D.; Ewing, W. C.; Hammond, K.; Jimenez-Halla, J. O. C.; Kramer, T.; Krummenacher, I.; Mies, J.; Phukan, A. K.; Vargas, A. Metal-free binding and coupling of carbon monoxide at a boron−boron triple bond. *Nat. Chem.* **2013**, *5* (12), 1025−1028.

(3) Shen, J.; Yap, G. P. A.; Theopold, K. H. Chromium Mediated Reductive Coupling of Isonitrile Forms Unusual Heterocycles. *J. Am. Chem. Soc.* **2014**, *136* (9), 3382−3384.

(4) Lu, W.; Li, Y.; Ganguly, R.; Kinjo, R. Crystalline Neutral Allenic Diborene. *Angew. Chem., Int. Ed.* **2017**, *56* (33), 9829−9832.

(5) Ghorai, S.; Jemmis, E. D. DFT Study of C−C and C−N Coupling on a Quintuple-Bonded Cr2 Template: MECP (Minimum Energy Crossing Point) Barriers Control Product Distribution. *Organometallics* **2020**, *39* (10), 1700−1709.

(6) Shen, J.; Yap, G. P. A.; Theopold, K. H. Binding and activation of small molecules by a quintuply bonded chromium dimer. *Chem. Commun.* **2014**, *50* (20), 2579−2581.

(7) Power, P. P. Main-group elements as transition metals. *Nature* **2010**, *463* (7278), 171−177.

(8) Hadlington, T. J.; Driess, M.; Jones, C. Low-valent group 14 element hydride chemistry: towards catalysis. *Chem. Soc. Rev.* **2018**, *47* (11), 4176−4197.

(9) Chu, T.; Nikonov, G. I. Oxidative Addition and Reductive Elimination at Main-Group Element Centers. *Chem. Rev.* **2018**, *118* (7), 3608−3680.

(10) Weetman, C.; Inoue, S. The Road Travelled: After Main-Group Elements as Transition Metals. *ChemCatChem* **2018**, *10* (19), 4213−4228.

(11) Légaré, M.-A.; Pranckevicius, C.; Braunschweig, H. Metallomimetic Chemistry of Boron. *Chem. Rev.* **2019**, *119* (14), 8231−8261.

(12) Reiter, D.; Holzner, R.; Porzelt, A.; Frisch, P.; Inoue, S. Silylated silicon−carbonyl complexes as mimics of ubiquitous transition-metal carbonyls. *Nat. Chem.* **2020**, *12* (12), 1131−1135.

(13) Ganesamoorthy, C.; Schoening, J.; Wölper, C.; Song, L.; Schreiner, P. R.; Schulz, S. A silicon−carbonyl complex stable at room temperature. *Nat. Chem.* **2020**, *12* (7), 608−614.

(14) Böhnke, J.; Braunschweig, H.; Dellermann, T.; Ewing, W. C.; Hammond, K.; Jimenez-Halla, J. O. C.; Kramer, T.; Mies, J. The Synthesis of B2 (SIDip) 2 and its Reactivity Between the Diboracumulenic and Diborynic Extremes. *Angew. Chem., Int. Ed.* **2015**, *54* (46), 13801−13805.

(15) Dangat, Y.; Vanka, K. Exploring the reducing role of boron: added insights from theory. *Dalton Trans.* **2016**, *45* (14), 5978−5988.

(16) Zhang, H.; Cao, Z.; Wu, W.; Mo, Y. The Transition-Metal-Like Behavior of B2 (NHC) 2 in the Activation of CO: HOMO−LUMO Swap Without Photoinduction. *Angew. Chem., Int. Ed.* **2018**, *57* (40), 13076−13081.

(17) Böhnke, J.; Braunschweig, H.; Dellermann, T.; Ewing, W. C.; Kramer, T.; Krummenacher, I.; Vargas, A. From an Electron-Rich Bis(boraketenimine) to an Electron-Poor Diborene. *Angew. Chem., Int. Ed.* **2015**, *54* (15), 4469−4473.

(18) Knizia, G. Intrinsic Atomic Orbitals: An Unbiased Bridge between Quantum Theory and Chemical Concepts. *J. Chem. Theory Comput.* **2013**, *9* (11), 4834−4843.

(19) Knizia, G.; Klein, J. E. Electron Flow in Reaction Mechanisms—Revealed from First Principles. *Angew. Chem., Int. Ed.* **2015**, *54* (18), 5518−5522.

(20) Wang, Y.; Kostenko, A.; Hadlington, T. J.; Luecke, M.-P.; Yao, S.; Driess, M. Silicon-mediated selective homo-and heterocoupling of carbon monoxide. *J. Am. Chem. Soc.* **2019**, *141* (1), 626−634.

(21) Yuvaraj, K.; Douair, I.; Paparo, A.; Maron, L.; Jones, C. Reductive Trimerization of CO to the Deltate Dianion Using Activated Magnesium(I) Compounds. *J. Am. Chem. Soc.* **2019**, *141* (22), 8764−8768.

(22) Chen, W.; Zhao, Y.; Xu, W.; Su, J.-H.; Shen, L.; Liu, L.; Wu, B.; Yang, X.-J. Reductive linear-and cyclo-trimerization of isocyanides using an Al−Al-bonded compound. *Chem. Commun.* **2019**, *55* (64), 9452−9455.

(23) Frenking, G.; Hermann, M.; Andrada, D. M.; Holzmann, N. Donor−acceptor bonding in novel low-coordinated compounds of

boron and group-14 atoms C−Sn. *Chem. Soc. Rev.* **2016**, *45* (4), 1129−1144.
(24) Zhao, L.; Hermann, M.; Holzmann, N.; Frenking, G. Dative bonding in main group compounds. *Coord. Chem. Rev.* **2017**, *344*, 163−204.
(25) Frisch, M. J.; Trucks, G. W.; Schlegel, H. B.; Scuseria, G. E.; Robb, M. A.; Cheeseman, J. R.; Scalmani, G.; Barone, V.; Mennucci, B.; Petersson, G. A.; Nakatsuji, H.; Caricato, M.; Li, X.; Hratchian, H. P.; Izmaylov, A. F.; Bloino, J.; Zheng, G.; Sonnenberg, J. L.; Hada, M.; Ehara, M.; Toyota, K.; Fukuda, R.; Hasegawa, J.; Ishida, M.; Nakajima, T.; Honda, Y.; Kitao, O.; Nakai, H.; Vreven, T.; Montgomery, J. A., Jr.; Peralta, J. E.; Ogliaro, F.; Bearpark, M. J.; Heyd, J.; Brothers, E. N.; Kudin, K. N.; Staroverov, V. N.; Kobayashi, R.; Normand, J.; Raghavachari, K.; Rendell, A. P.; Burant, J. C.; Iyengar, S. S.; Tomasi, J.; Cossi, M.; Rega, N.; Millam, N. J.; Klene, M.; Knox, J. E.; Cross, J. B.; Bakken, V.; Adamo, C.; Jaramillo, J.; Gomperts, R.; Stratmann, R. E.; Yazyev, O.; Austin, A. J.; Cammi, R.; Pomelli, C.; Ochterski, J. W.; Martin, R. L.; Morokuma, K.; Zakrzewski, V. G.; Voth, G. A.; Salvador, P.; Dannenberg, J. J.; Dapprich, S.; Daniels, A. D.; Farkas, Ö.; Foresman, J. B.; Ortiz, J. V.; Cioslowski, J.; Fox, D. J. *Gaussian 09*; Gaussian, Inc.: Wallingford, CT, USA, 2009.
(26) Zhao, Y.; Truhlar, D. The M06 suite of density functionals for main group thermochemistry, thermochemical kinetics, noncovalent interactions, excited states, and transition elements: two new functionals and systematic testing of four M06-class functionals and 12 other functionals. *Theor. Chem. Acc.* **2008**, *120* (1−3), 215−241.
(27) Zhao, Y.; Truhlar, D. G. Density functionals with broad applicability in chemistry. *Acc. Chem. Res.* **2008**, *41* (2), 157−167.
(28) Bickelhaupt, F. M.; Baerends, E. J. Kohn-Sham Density Functional Theory: Predicting and Understanding Chemistry. *Reviews in Computational Chemistry, Volume 15* **2007**, 1−86.
(29) Te Velde, G.; Bickelhaupt, F. M.; Baerends, E. J.; Fonseca Guerra, C.; van Gisbergen, S. J.; Snijders, J. G.; Ziegler, T. Chemistry with ADF. *J. Comput. Chem.* **2001**, *22* (9), 931−967.
(30) Kahn, B. E.; Rieke, R. D. Carbonyl coupling reactions using transition metals, lanthanides, and actinides. *Chem. Rev.* **1988**, *88* (5), 733−745.
(31) Summerscales, O. T.; Cloke, F. G. N.; Hitchcock, P. B.; Green, J. C.; Hazari, N. Reductive Cyclotrimerization of Carbon Monoxide to the Deltate Dianion by an Organometallic Uranium Complex. *Science* **2006**, *311* (5762), 829−831.
(32) Summerscales, O. T.; Cloke, F. G. N.; Hitchcock, P. B.; Green, J. C.; Hazari, N. Reductive Cyclotetramerization of CO to Squarate by a U(III) Complex: The X-ray Crystal Structure of [(U (η-C8H6{SiiPr3−1,4}2)(η-C5Me4H)]2(μ-η2: η2-C4O4). *J. Am. Chem. Soc.* **2006**, *128* (30), 9602−9603.
(33) Watanabe, T.; Ishida, Y.; Matsuo, T.; Kawaguchi, H. Reductive Coupling of Six Carbon Monoxides by a Ditantalum Hydride Complex. *J. Am. Chem. Soc.* **2009**, *131* (10), 3474−3475.
(34) McKay, D.; Frey, A. S.; Green, J. C.; Cloke, F. G. N.; Maron, L. Computational insight into the reductive oligomerisation of CO at uranium (iii) mixed-sandwich complexes. *Chem. Commun.* **2012**, *48* (34), 4118−4120.
(35) Wu, J.; Fanwick, P. E.; Kubiak, C. P. Lewis acid-promoted carbon-carbon bond formation between bridging isocyanides. *J. Am. Chem. Soc.* **1988**, *110* (4), 1319−1321.
(36) Li, H.; Feng, H.; Sun, W.; King, R. B.; Schaefer, H. F. Extreme Metal Carbonyl Back Bonding in Cyclopentadienylthorium Carbonyls Generates Bridging C2O2 Ligands by Carbonyl Coupling. *Inorg. Chem.* **2013**, *52* (12), 6893−6904.
(37) Kong, R. Y.; Crimmin, M. R. Cooperative strategies for CO homologation. *Dalton Trans.* **2020**, *49*, 16587.
(38) Rosenthal, U. Carbon Monoxide Coupling Reactions: A New Concept for the Formation of Hexahydroxybenzene. *Chem. - Eur. J.* **2020**, *26* (64), 14507−14511.
(39) Paparo, A.; Yuvaraj, K.; Matthews, A. J. R.; Douair, I.; Maron, L.; Jones, C. Reductive Hexamerization of CO Involving Cooperativity Between Magnesium(I) Reductants and [Mo(CO)6]: Synthesis of Well-Defined Magnesium Benzenehexolate Complexes. *Angew. Chem., Int. Ed.* **2021**, *60*, 630−634.
(40) Lavallo, V.; Canac, Y.; Präsang, C.; Donnadieu, B.; Bertrand, G. Stable Cyclic (Alkyl)(Amino)Carbenes as Rigid or Flexible, Bulky, Electron-Rich Ligands for Transition-Metal Catalysts: A Quaternary Carbon Atom Makes the Difference. *Angew. Chem., Int. Ed.* **2005**, *44* (35), 5705−5709.
(41) Soleilhavoup, M.; Bertrand, G. Cyclic (Alkyl)(Amino)Carbenes (CAACs): Stable Carbenes on the Rise. *Acc. Chem. Res.* **2015**, *48* (2), 256−266.
(42) Huynh, H. V. Electronic Properties of N-Heterocyclic Carbenes and Their Experimental Determination. *Chem. Rev.* **2018**, *118* (19), 9457−9492.
(43) Celik, M. A.; Sure, R.; Klein, S.; Kinjo, R.; Bertrand, G.; Frenking, G. Borylene Complexes (BH)L2 and Nitrogen Cation Complexes (N+)L2: Isoelectronic Homologues of Carbones CL2. *Chem. - Eur. J.* **2012**, *18* (18), 5676−5692.
(44) Arduengo, A. J.; Harlow, R. L.; Kline, M. A stable crystalline carbene. *J. Am. Chem. Soc.* **1991**, *113* (1), 361−363.
(45) Krogh-Jespersen, K.; Cremer, D.; Dill, J. D.; Pople, J. A.; Schleyer, P. R. Aromaticity in small rings containing boron and carbon, ((CH)2(BH)n, n = 1,2): comarisons with isoelectronic carbocations. The decisive roles of orbital mixing and nonbonded 1,3-interactions in the structures of four-membered rings. *J. Am. Chem. Soc.* **1981**, *103* (10), 2589−2594.
(46) Budzelaar, P. H. M.; Krogh-Jespersen, K.; Clark, T.; Schleyer, P. v. R. Remarkable structures of C2B2H4 isomers. *J. Am. Chem. Soc.* **1985**, *107* (9), 2773−2779.
(47) Balci, M.; McKee, M. L.; Schleyer, P. v. R. Theoretical Study of Tetramethyl- and Tetra-tert-butyl-Substituted Cyclobutadiene and Tetrahedrane. *J. Phys. Chem. A* **2000**, *104* (6), 1246−1255.
(48) McKee, W. C.; Wu, J. I.; Hofmann, M.; Berndt, A.; Schleyer, P. v. R. Why Do Two π-Electron Four-Membered Hückel Rings Pucker? *Org. Lett.* **2012**, *14* (22), 5712−5715.
(49) Arrowsmith, M.; Böhnke, J.; Braunschweig, H.; Celik, M. A.; Claes, C.; Ewing, W. C.; Krummenacher, I.; Lubitz, K.; Schneider, C. Neutral Diboron Analogues of Archetypal Aromatic Species by Spontaneous Cycloaddition. *Angew. Chem., Int. Ed.* **2016**, *55* (37), 11271−11275.
(50) Ghorai, S.; Jemmis, E. D. A DFT Study on the Stabilization of the B≡ B Triple Bond in a Metallaborocycle: Contrasting Electronic Structures of Boron and Carbon Analogues. *Chem. - Eur. J.* **2017**, *23* (41), 9746−9751.
(51) Brown, Z. D.; Vasko, P.; Fettinger, J. C.; Tuononen, H. M.; Power, P. P. A Germanium Isocyanide Complex Featuring (n → π*) Back-Bonding and Its Conversion to a Hydride/Cyanide Product via C−H Bond Activation under Mild Conditions. *J. Am. Chem. Soc.* **2012**, *134* (9), 4045−4048.
(52) Brown, Z. D.; Power, P. P. Mechanisms of reactions of open-shell, heavier group 14 derivatives with small molecules: n− π* back-bonding in isocyanide complexes, C−H activation under ambient conditions, CO coupling, and ancillary molecular interactions. *Inorg. Chem.* **2013**, *52* (11), 6248−6259.
(53) Takeuchi, K.; Ichinohe, M.; Sekiguchi, A. A New Disilene with π-Accepting Groups from the Reaction of Disilyne RSi≡SiR (R = SiiPr[CH(SiMe3)2]) with Isocyanides. *J. Am. Chem. Soc.* **2012**, *134* (6), 2954−2957.
(54) Wang, X.; Zhu, Z.; Peng, Y.; Lei, H.; Fettinger, J. C.; Power, P. P. Room-Temperature Reaction of Carbon Monoxide with a Stable Diarylgermylene. *J. Am. Chem. Soc.* **2009**, *131* (20), 6912−6913.
(55) Ghorai, S.; Jemmis, E. D. Structures and bonding in [L]M(μ-CCR)2M[L] and [L]M(μ-RC4R)M[L]: requirements for C−C coupling. *Dalton Trans.* **2020**, *49* (16), 5157−5166.
(56) Légaré, M.-A.; Rang, M.; Bélanger-Chabot, G.; Schweizer, J. I.; Krummenacher, I.; Bertermann, R.; Arrowsmith, M.; Holthausen, M. C.; Braunschweig, H. The reductive coupling of dinitrogen. *Science* **2019**, *363* (6433), 1329−1332.

https://doi.org/10.1021/acs.jpca.1c05185
J. Phys. Chem. A 2021, 125, 7207−7216

(57) Zhou, J.; Liu, L. L.; Cao, L. L.; Stephan, D. W. Reductive Coupling and Loss of N2 from Magnesium Diazomethane Derivatives. *Chem. - Eur. J.* **2018**, *24* (34), 8589−8595.

https://doi.org/10.1021/acs.jpca.1c05185
J. Phys. Chem. A 2021, 125, 7207−7216